Cell death mechanisms during follicular atresia in *Dipetalogaster maxima*, a vector of Chagas' disease (Hemiptera:Reduviidae)

Silvina A. Aguirre, Patricia Pons, Beatriz P. Settembrini, Daniela Arroyo, Lilián E. Canavoso

PII: S0022-1910(13)00060-7
DOI: http://dx.doi.org/10.1016/j.jinsphys.2013.03.001
Reference: IP 3062

To appear in: *Journal of Insect Physiology*

Received Date: 30 November 2012
Revised Date: 27 February 2013
Accepted Date: 5 March 2013

Please cite this article as: Aguirre, S.A., Pons, P., Settembrini, B.P., Arroyo, D., Canavoso, L.E., Cell death mechanisms during follicular atresia in *Dipetalogaster maxima*, a vector of Chagas' disease (Hemiptera:Reduviidae), *Journal of Insect Physiology* (2013), doi: http://dx.doi.org/10.1016/j.jinsphys.2013.03.001

Cell death mechanisms during follicular atresia in *Dipetalogaster maxima*, a vector of Chagas' disease (Hemiptera:Reduviidae).

Silvina A. Aguirre[1], Patricia Pons[2], Beatriz P. Settembrini[3, #], Daniela Arroyo[1], Lilián E. Canavoso[1, #, *].

[1] Departamento de Bioquímica Clínica, Centro de Investigaciones en Bioquímica Clínica e Inmunología (CIBICI-CONICET). Facultad de Ciencias Químicas-Universidad Nacional de Córdoba. Córdoba, CP 5000, Argentina.

[2] Centro de Microscopía Electrónica, Instituto de Investigaciones en Ciencias de la Salud (INICSA-CONICET), Facultad de Ciencias Médicas-Universidad Nacional de Córdoba. Córdoba, CP 5000, Argentina.

[3] Museo Argentino de Ciencias Naturales-CONICET, Buenos Aires, Argentina.

* Corresponding author. Tel. + 54 351 434-4974; Fax: + 54 351 433-3048.

E-mail address: lcanavo@mail.fcq.unc.edu.ar

[#] Members of the CIC-CONICET-Argentina

Abstract

In this work we have analyzed the involvement of cell death pathways during the process of follicular atresia in the hematophagous insect vector *Dipetalogaster maxima*. Standardized insect rearing conditions were established to induce a gradual follicular degeneration stage by depriving females of blood meal during post-vitellogenesis. We first characterized the morpho-histological and ultrastructural changes of the ovarian tissue at early and late follicular atresia by light and transmission electron microscopy. Apoptosis was investigated by DAPI nuclear staining, TUNEL labeling and the detection of active caspase-3 by immunofluorescence. Autophagy was assessed by the measurement of acid phosphatase activity in ovarian homogenates and monitored by the detection of the specific marker of autophagic compartments, LC3. High levels of acid phosphatase activity were detected at all atretic stages. However, follicular cells of follicles undergoing incipient degeneration in early atresia exhibited features of apoptosis such as chromatin condensation, DNA fragmentation and the presence of active caspase-3. The ultrastructural findings and the increased levels of LC3-II found at late follicular atresia supported the relevance of autophagy at this atretic stage, although the extent of autophagosome formation demonstrated that this cell death pathway also occurred at early atresia. In late atresia, follicular cells also displayed more drastic changes compatible with necrosis. Taken together, results showed that apoptosis, autophagy and necrosis were operative during follicular atresia in *D. maxima*. Moreover, it was shown that the relevance of these cell death mechanisms correlates with the time elapsed since the onset of the degenerative process.

Keywords: *Dipetalogaster maxima*, reproduction, follicular atresia, apoptosis, autophagy, necrosis.

1. Introduction

When insects face unfavorable physiological or environmental conditions, the ovarian tissue undergoes changes that lead to the degeneration of some follicles to an atretic stage. During this process, termed follicular atresia, oocytes are resorbed ("oosorption") instead of continuing their maturation (Bell and Bhom, 1975). Oosorption is usually triggered by shortage of food and in most instances, is considered an adaptive mechanism directed to recoup resources which in turn, would supply physiological functions to either, increase female lifespan or facilitate its future reproductive success (Bell y Bhom, 1975; Moore and Attisano, 2011).

In mammals, ovarian cell death plays a critical role for the homeostasis of ovarian function since a large majority of follicles are eliminated by the degenerative process of atresia (Tilly, 1996, 2001). Thus, granulose cells undergo apoptosis in atretic follicles earlier than theca cells and oocytes. Factors associated with apoptosis expressed by ovarian cells were shown to be crucial for the precise coordination of atresia (Matsuda et al., 2012).

According to the morphological criteria, cell death is classified in apoptosis, autophagy and necrosis (Galluzzi et al., 2007; Kroemer et al., 2009). Apoptosis is an evolutionary conserved and genetically regulated mechanism whose execution is associated with chromatin condensation, DNA fragmentation and the presence of apoptotic bodies (Kerr et al., 1972; Taatjes et al., 2008). The effector molecules of the apoptotic machinery are a family of cysteine aspartate-specific peptidases termed caspases. After the cells received a pro-apoptotic stimulus, caspases are activated to specifically process several substrates implicated in apoptosis (Köhler, 2002; Lavrik et al., 2005). On the other hand, during autophagic cell death, part of the cytoplasm is sequestered within double-membrane vacuoles or autophagosomes, and finally digested by lysosomal hydrolases (Eskelinen, 2005). Autophagy regulates aging, organelle turnover and

mobilization of metabolic resources upon starvation (Klionsky et al., 2008; Backues and Klionsky, 2011). Necrosis, the third type of cell death, is usually considered to be uncontrolled and it is likely the result of a severe ATP depletion which causes plasma membrane break down and inflammation. Necrosis lacks specific biochemical markers but can be detected by electron microscopy (Golstein and Kroemer, 2005, 2007; Galluzzi et al., 2007).

In insects, the biochemical and cellular events involved in follicular atresia have been analyzed in few species (Uchida et al., 2004; Clifton and Noriega, 2011; Medeiros et al., 2011). Moreover, factors acting in their regulation remain still unclear. In the developing ovaries of the mosquito *Culex pipiens pallens,* follicular atresia is needed to adjust the size of the egg batch to available nutrients by the elimination of the follicular epithelial cells via activation of apoptosis (Uchida et al., 2004). Atretic follicles of *Dacus oleae,* detected exclusively during mid-oogenesis, exhibited nurse cells with chromatin condensation, DNA fragmentation and actin cytoskeleton disorganization (Nezis et al., 2006). Moreover, during mid and late oogenesis of *Drosophila virilis* and *Ceratitis capitata*, both apoptosis and autophagy seem to operate in concert to achieve the elimination of degenerated nurse cells and abnormal egg chambers (Velentzas et al., 2007a, b).

Triatomines are obligatory hematophagous insects with relevance in public health since they are vectors of the parasite *Trypanosoma cruzi*, the etiological agent of Chagas' disease (Coura and Viñas, 2010). In the females of triatomines, atresia is frequently observed during starvation or when the size of blood meal failed to promote vitellogenesis. However, it has received little attention and the few available studies are mainly restricted to *Rhodnius prolixus* (Wigglesworth, 1943; Huebner and Anderson, 1972; Stoka et al., 1987). In this species, the histological characterization of atretic follicles was recently reported (Medeiros et al., 2011).

The females of the triatomine *Dipetalogaster maxima* are useful models to study the biochemical and cellular events during the processes of vitellogenesis and follicular atresia (Aguirre et al., 2008, 2011). Under standardized conditions, the anautogenous female takes a large blood meal to elicit vitellogenesis. Because ovarioles are asynchronous to each other, the first oviposition period lasts 25-28 days after blood intake. Thereafter, ovaries enter into a post-vitellogenic stage during which, some terminal follicles become atretic and the oocytes are resorbed. In opposition to most species previously analyzed, in which the onset of atresia occurs very fast, the morphological changes of ovarian tissue during post-vitellogenesis in *D. maxima* are gradual allowing to distinguishing an early and a late stage of follicular atresia (Aguirre et al., 2011). The follicle degeneration and oocyte resorption may cease if female receives another blood meal, which in triatomines is necessary at least for the production of a second batch of eggs (Stoka et al., 1987). At a biochemical level, follicular atresia was recently characterized (Aguirre et al., 2011).

In order to improve our understanding of the biology of reproduction of the hematophagous vectors of Chagas' disease, in this work we have analyzed the involvement of cell death pathways during the process of follicular atresia in *D. maxima*. We demonstrated for the first time that apoptosis, autophagy and necrosis are operative during follicular atresia. Moreover, it was shown that the relevance of the different cell death mechanisms correlates with the time elapsed since the onset of the degenerative process.

2. Materials and Methods

2.1 Chemicals

4',6-diamidino-2-phenylindole (DAPI) (Molecular Probes, OR, USA), Tissue-Tek embedding medium (OCT) (Miles, Elkhart, IN, USA), Fluorsave (Calbiochem, Darmstadt, Germany), DPX Mountant for histology (Fluka, BioChemika, Switzerland), enhanced chemiluminiscence (ECL) detection kit (PerkinElmer, Waltham, MA, USA), cleaved caspase-3 antibody and LC3A/B antibody raised in rabbit (Cell Signaling Technology, Danvers, MA, USA), and in situ cell death detection Kit-POD (Boehringer Mannheim, Germany) were from indicated commercial sources. Horseradish peroxidase (HRP)-conjugated goat anti-rabbit IgG, bovine serum albumin (BSA) and all the remaining chemicals were from Sigma-Aldrich (St. Louis, MO, USA).

2.2. Insects

Insects were taken from a colony of anautogenous *D. maxima,* which is maintained under standardized conditions (28^{o}C, 70% humidity, 8:16 h light:dark photoperiod) and fed every two weeks on hen blood (Canavoso and Rubiolo, 1995).

For the experiments, males and females were separated before feeding at the last nymphal instar. Newly-emerged females were segregated individually and placed with two recently fed males for a period of 48 h and daily checked for mating by observation of the spermatophore. Mated females were maintained in individual containers until they were able to feed a blood meal (days 10-12 post-ecdysis) (Aguirre et al., 2008). Under these conditions, females were daily monitored and both, the beginning and the end of the oviposition period, which was confirmed if females did not lay eggs during five consecutive days, were recorded. Females were also monitored for at least 32 days after the end of the oviposition (post-vitellogenesis), unless

otherwise stated. During post-vitellogenesis females did not receive any further blood meal (Aguirre et al., 2011).

For the studies, ovaries were sampled from females at representative days of the reproductive cycle: (a) pre-vitellogenesis (day 2 post-ecdysis, unfed period); (b) vitellogenesis (days 4-6 post-blood feeding); (c) post-vitellogenesis (days 10-12 and days 30-32 after the end of oviposition for early and late atresia, respectively) according to Aguirre et al. (2011). To determine acid phosphatase activity, additional time points during post-vitellogenesis (days 6-8 and days 40-45) were tested.

2.3. Sampling of ovaries

Ovaries at different times of the reproductive cycle were carefully dissected out and washed three times with phosphate buffer saline (PBS, 6.6 mM Na_2HPO_4/KH_2PO_4, 150 mM NaCl, pH 7.4) and fixed in 4 % paraformaldehyde in PBS. To obtain paraffin sections, fixed ovaries were dehydrated, embedded in paraffin and processed for histological studies. Also, fixed ovaries were transferred into sucrose/PBS and then, embedded in OCT and frozen in liquid nitrogen (Fruttero et al., 2009). Thereafter, cryosections (8 µm thick) were obtained with a Leica CM1510 cryostat (Leica Microsystems, Wetzlar, Germany) and placed onto poly-L-lysine-treated glass slides.

2.4. Conventional light and transmission electron microscopy

In order to study the morphological changes in the ovary during early and late follicular atresia, ovaries were dissected out and fixed as described previously in 2.3. For light microscopy, tissue sections were stained with hematoxylin-eosin (H&E) and examined with a Zeiss

microscope (Aguirre et al., 2008). For ultrastructural analysis, ovaries were fixed for 4 h at 4 ^{o}C (2.5 % glutaraldehyde, 2 % paraformaldehyde, 0.1 M sodium cacodylate, pH 7.2) and then post-fixed with 1 % osmium tetroxide in cacodylate buffer at 4 ^{o}C. Samples were dehydrated, embedded onto an Araldite resine to obtain semi-thin sections which were stained with toluidine blue. Ultra-thin sections (80 nm) were counterstained with a saturaded solution of uranyl acetate and 1 % lead citrate and viewed with a Leo 906e Transmission Electron Microscope.

2.5. DAPI nuclear staining

Nuclear morphology was studied by DAPI staining. Ovaries at early and late follicular atresia stages were isolated and cryostat tissue sections were obtained as described in 2.3. For DAPI staining slides were incubated with 300 nM DAPI in PBS in a humid chamber at 37 ^{o}C for 40 min in the dark (Li et al., 2000). After three washes with PBS, slides were rinsed with PBS, air-dried, mounted in Fluorsave and observed with an Eclipse TE2000-U microscope (Nikon, Tokyo, Japan), equipped with appropriate filters (excitation 435–480 nm/emission 340–380 nm). Images were captured with a Nikon Digital Sight DS-U1 camera and processed with ACT-2U version 1.51.116.256 software.

2.6. TUNEL labeling of fragmented DNA

The TUNEL (terminal transferase-mediated dUTP nick-end labeling) assay was performed for detection of fragmented DNA (Gavrieli et al., 1992). Briefly, ovaries at vitellogenesis, early and late follicular atresia stages were isolated and processed as described in 2.3. Deparaffinized tissue sections were rehydrated, blocked for endogen peroxidase activity and then treated with proteinase K for permeabilization. After the washes with PBS, the TUNEL assay was run using

an apoptosis detection kit which contained an anti-dUTP antibody labeled with peroxidase (POD) according to manufacturer's instructions.

2.7. Detection of active caspase-3 by immunofluorescence

Cryostat sections of ovaries in vitellogenesis and at early and late follicular atresia stages were obtained as described in 2.3 and placed onto glass slides. For immunofluorescence assays, the slides were blocked with 1 % BSA, 0.1 % Triton X-100, 5 % fetal bovine serum (FBS) in PBS and then incubated overnight at 4 ^{o}C with an anti-cleaved caspase-3 antibody (1:800). Slides were washed with PBS and then incubated with Alexa Fluor 568-conjugated goat anti-rabbit IgG (1:500) for 1 h, at 37 ^{o}C in the dark. The two antibodies were diluted in PBS containing 1 % BSA. Nuclei were stained with 300 nM DAPI as stated in 2.5. After that, the slides were rinsed in distilled water, air-dried, mounted in Fluorsave and observed with an Olympus FV1000 laser scanning confocal microscope (Olympus, Tokyo, Japan) equipped with 405 nm and 543 nm lasers. Images were acquired and processed with FluoView FV1000 version 1.7.1.0 software.

2.8. Acid phosphatase assay

The activity of acid phosphatase, an enzyme associated to autophagic degradation of tissues, was assayed by measuring the hydrolysis of *p*-nitrophenyl phosphate (pNPP) (Oliveira et al., 2006). Briefly, ovaries sampled at different stages of the reproductive cycle of *D. maxima* were homogenized in 20 mM sodium acetate buffer pH 4.0, containing 10 mM dithiotreitol (DTT), 10 mM Na_2EDTA, 2 mM phenylmethyl-sulfonyl fluoride (PMSF), 0.01 mM pepstatin and 50 µM soybean trypsin inhibitor (SBTI). After centrifugation (14,000 x*g*, 5 min, 4 ^{o}C),

supernatants were collected and immediately assayed for acid phosphatase activity, before protein determination. The enzymatic activity was measured by incubating 30 µg of protein homogenates in a reaction medium containing 5 mM pNPP, 10 mM DTT, 10 mM Na_2EDTA in 20 mM sodium acetate buffer, pH 4.0 at 37 ^{o}C. The reactions proceeded for 30 min and were stopped by the addition of 4 N NaOH. The amount of *p*-nitrophenol (pNP) released was registered at 405 nm and calculated on the basis of a standard curve. Specific activity was expressed as nmol pNP/mg protein homogenate/min. Controls without ovary homogenates were used as blanks.

2.9. Detection of LC3 as a marker of autophagy

In order to assess the involvement of autophagy during follicular atresia of *D. maxima,* we analyzed by immunofluorescence the presence of microtubule-associated protein 1 light chain 3 (LC3), a marker of autophagy (Kabeya et al., 2000). In addition, the conversion of LC3-I to LC3-II form was determined by western blot assays.

For the immnoflourescence assays, ovaries during pre-vitellogenesis, vitellogenesis and at early and late follicular atresia stages were dissected out and cryostat tissue sections were obtained as described previously in 2.3. The slides were blocked as stated in 2.7, washed with PBS and then incubated with an anti-LC3 antibody (1:400), overnight at 4 ^{o}C. Slides were washed three times with PBS and then incubated with the Alexa Fluor 568-conjugated goat anti-rabbit IgG (1:500) for 1 h at 37 ^{o}C. Both, the first and the second antibodies were diluted in PBS containing 1 % BSA. Finally, the slides were rinsed with distilled water, air-dried, mounted in Fluorsave and observed with an Olympus FV1000 laser scanning confocal microscope

(Olympus, Tokyo, Japan) equipped with a 548 nm laser. Images were acquired and processed with FluoView FV1000 version 1.7.1.0 software.

To carry out the western blot analysis, ovaries from *D. maxima* were homogenized with ice-cold lysis buffer solution (60 mM Tris-HCl, 25 % glycerol, 2 % sodium docecyl sulfate (SDS), 14.4 mM 2-mercaptoethanol, 0.1 % bromophenol blue, pH 6.8). After three cycles of sonication (15 sec each one), the homogenates were boiled for 5 min and then centrifuged for 10 min at 10,000 x*g*. Equal volumes of each supernatant fraction were separated by SDS-PAGE (13 %) and then transferred onto a nitrocellulose membrane for 1h. Western blot was performed according to Towbin et al. (1979). Blocking steps were carried out with TBS-5 % non-fat milk (TBS: 10 mM Tris-HCl, 150 mM NaCl). Primary and secondary antibodies were diluted in TBS-0.1 % Tween 20 containing 5 % BSA and used in the incubations as following: anti-LC3 antibody (1:1000, overnight, at 4 °C with gentle shaking) and HRP-conjugated goat anti-rabbit IgG (1:2000, for 1 h and at room temperature). The immunoreactive bands were detected by ECL.

2.10. Statistical analysis

Morphometric measurements of ovarioles and follicles were individually performed using six females for each stage of the reproductive cycle. For enzymatic assays, four to six independent experiments were carried out, including at each point the ovaries from two females. The data were registered by duplicate. Graphs and statistical tests were performed using GraphPad Prism and GraphPad Instat 3.0 computer programs. Results were expressed as mean ± SEM. Analysis of the multiple intergroup differences was conducted by one way ANOVA. As post-test, the

Student-Newman-Keuls multiple comparisons test was used. Differences were considered significant at P value < 0.05.

3. Results

3.1. Morphological, histological and ultrastructural features of follicular atresia

In *D. maxima,* ovarioles in early atresia showed an average length of about 2.82 mm. They maintained some degree of asynchronous development as revealed by the presence of terminal follicles of variable length (from 0.6 to 0.9 mm) (Fig. 1). One of the main features of this stage was the presence of developed terminal follicles coexisting with follicles undergoing incipient degeneration as well as with resorbed oocytes. The latter ones were evidenced as yellow-pigmented bodies (Fig. 2A).

Histological examination of the follicles undergoing incipient degeneration revealed the progressive loss of the normal pattern of the follicular epithelium (Fig. 2B). Groups of follicle cells appeared as rounded shrunken masses, showing intense eosinophilia of the cytoplasm and dense purple chromatin condensation. Instead, other follicle cells contained euchromatic nuclei (Fig. 2B). The condensation of chromatin was also visible in nuclei stained with DAPI (Fig. 2C). The pattern of condensation observed in nuclei with both stainings suggests that in early atresia, follicular cells are undergoing apoptosis (Fig. 2B-C). Alterations in the morphology of the follicular epithelium, which included vacuolization of the cytoplasm and chromatin condensation, were observed in semi-thin sections of follicles undergoing incipient degeneration stained with toluidine blue (Fig. 2D). Examination of follicular cells in early atresia by transmission electron microscopy (TEM) revealed morphological features typical of apoptosis, such as early nuclear chromatin condensation into dense masses at the nuclear periphery (Fig. 2E). In addition, apoptotic bodies inside adjacent cells were observed (Fig. 2F). Altogether, these results suggest the participation of apoptosis in early atresia.

On the contrary, in ovarioles at late follicular atresia stage the asynchronous development is lost, they became noticeably smaller (about 2.36 mm) and all of them showed resorbed oocytes, as an expression of a generalized process of degeneration (Fig. 1). At this stage no follicles undergoing incipient degeneration were observed (Fig. 3A). The small terminal follicles lost the typical columnar arrangement of the follicular epithelium and no evidence of chromatin condensation was observed (Fig. 3B-C). TEM observations of the follicular cells revealed the presence of large vacuoles containing remnants of organelles (cisternae of the endoplasmic reticulum and mitochondria) as well as multilamellar bodies in the vicinity of these vacuoles (Fig. 3D). Also, the follicular epithelium showed extended areas of lysed cytoplasm (result not shown). Altogether, these findings were indicative of an autophagic process. However, in late atresia, cells also displayed more drastic changes including dilations of nuclear membrane, mitochondria lacking cristae and signs of necrosis such as electron lucent vacuoles (Fig. 3E-F).

3.2. Cell death during early follicular atresia in D. maxima: *apoptosis*

During early atresia, the detection of *in situ* apoptosis in ovarian tissue sections showed that the majority of TUNEL-positive signals were confined to follicular cells of follicles undergoing incipient degeneration (Fig. 4A). No positive signal for TUNEL was detected either in vitellogenic follicles (Fig. 4B) or in the small terminal follicles at late atresia stage (results not shown).

Since activated caspases mediate many of the typical changes in apoptotic cells, we performed immunofluorescense assays to detect the presence of active caspase-3, the main executioner caspase, during the process of follicular atresia. As shown in Fig. 5A, at early atresia stage, an intense fluorescent signal for active caspase-3 was found in the follicular epithelium of

those follicles undergoing incipient degeneration. Moreover, such follicular cells evidenced a chromatin condensation pattern when nuclei were stained with DAPI (Fig. 5B-C). On the contrary, no active caspase-3 was detected either at late follicular atresia stage or at vitellogenesis (results not shown). Altogether, these results indicate that the pathway through which apoptotic mechanisms operate is mediated by active caspases.

3.3. Cell death during late follicular atresia in D. maxima: *autophagy*

Ultrastructural studies performed in females at late atresia stage demonstrated the presence of autophagosomes as well as morphological changes compatible with an active autophagic process (Fig. 3D). Since acid phosphatase is a lysosomal hydrolase associated with autophagy, we measured the activity of this enzyme in ovarian tissues sampled throughout the reproductive cycle of *D. maxima* (Fig. 6). Although in all atretic samples the activity of acid phosphatase was significantly higher than those registered at pre-vitellogenesis and vitellogenesis, the highest activity level was detected at days 10-12 post-vitellogenesis. It is noteworthy that in an advanced degeneration stage (days 40-45 post-vitellogenesis), the activity of acid phosphatase was significantly lower than that observed at the early atretic stage. As shown in Fig. 6, homogenates at pre-vitellogenic and vitellogenic stages displayed comparably lower levels of the enzyme activity. Taken together, these results suggested that the process of follicular atresia in *D. maxima* is encompassed by an important autophagic activity.

To demonstrate that autophagy is activated during atresia, we investigated this cell death mechanism by the detection of a specific marker, LC3. Since the conversion of LC3-I (cytosolic form, 18 kDa) to LC3-II (membrane-bound autophagosome, 16 kDa) closely correlates with the extent of autophagosome formation; we first analyzed the levels of LC3-II during follicular

atresia by western blot. Although ovarian homogenates at early and late atresia stages showed an important increase of the immunoreactive band of LC3-II, when compared to those found at pre-vitellogenesis and vitellogenesis (Fig. 7A), such LC3-II formation was more remarkable in samples in late atresia.

On the other hand, we also tested the presence of LC3 by immunofluorescence on cryosections of ovarian tissues. In agreement with the western blot assays, at early stage of atresia only follicular cells of follicles undergoing incipient degeneration displayed a punctate fluorescent pattern. Such pattern represents the membrane-bound form of LC3 or LC3-II, a fact which is consistent with autophagy. Moreover, this pattern of LC3 immunoreactivity was absent in follicles displaying some degree of development (Fig. 7B). Remarkably, at late atresia stage, an increase in punctate signal of LC3-II was expanded to most of the follicular cells, indicating the abundance of autophagosomes (Fig. 7C). Overall, these results reinforced the involvement of autophagy as a relevant cell death mechanism during the advanced atresia.

When autophagy was assessed at pre-vitellogenesis, the follicular cells displayed a weak and dispersed LC3-I-like immunoreactivity, while no immunopositive signal for LC3-II was detected. However, a scarce immunolabeling pattern of LC3-II was observed in vitellogenic follicles (Fig. 7D-E). Taken together, these results indicate that at pre-vitellogenesis and vitellogenesis, autophagy has not been significantly induced.

4. Discussion

In mammals, follicular atresia is a complex physiological process in which biochemical and cellular events converge to eliminate follicles instead of promoting their maturation (Tilly, 1996, 2001; Matsuda et al., 2012). In insects, it is known that in *Drosophila melanogaster* and other higher dipterans, nurse and follicle cells undergo programmed cell death during the developmental stages of oogenesis (Nezis et al., 2000, 2002, 2005). On the contrary, the occurrence of cell death during the progress of follicular atresia has been explored in few species (Uchida et al., 2004; Clifton and Noriega, 2011; Medeiros et al., 2011).

In *D. maxima*, deprivation of blood meal during post-vitellogenesis led to the degeneration of some follicles to an atretic stage (Aguirre et al., 2011). In this work, we found that apoptosis was a relevant cell death mechanism operating at early stages of this degenerative process, which in turn was confined to those follicles undergoing incipient degeneration (Fig. 3-4). Caspases play a major role in the initiation and execution phases of apoptosis. Once activated, these enzymes mediate many of the typical biochemical and morphological changes in apoptotic cells. Caspase-3, the main executioner caspase, has been shown to be essential for DNA fragmentation as well as for chromatin condensation. Hence, the detection of active caspase-3 can be used as a biochemical marker for apoptosis (Köhler et al., 2002). Our results demonstrated that at the early atretic stage, the pathway through which apoptotic mechanisms operate was mediated by caspases, since immunofluorescence assays revealed the presence of active caspase-3 (Fig. 5). Similarly, during mid-oogenesis of *D. virilis*, spontaneously degenerated egg chambers exhibited apoptotic nurse cells with high levels of caspase activity (Velentzas et al., 2007a). Moreover, during stages 8 to 9 of *Bombix mori* late vitellogenesis, the nurse cell nuclei showed highly condensed chromatin, fragmented DNA and the occurrence of activated caspases (Mpakou et al.,

2006). In *D. melanogaster*, the atretic egg chambers found during mid-oogenesis contained degenerated nurse cells exhibiting morphological signs of apoptosis and the presence of activated casapase-3 (Nezis et al., 2009). It has been proposed that in degenerating follicles of *C. p. pallens*, activation of a cascade of caspases in surviving epithelial cells initiates their own death by apoptosis (Uchida et al., 2004). The hormonal basis of apoptosis during follicular atresia is not completely understood. In *D. melanogaster*, it seems that 20-hydroxyecdysone and juvenile hormone (JH) induce and suppress apoptosis of nurse cells at mid-oogenesis, respectively (Soller et al., 1999; Terashima et al., 2005). Recently, it was also proposed that JH plays a primary role on reproductive trade-offs in *Aedes aegypti* during the pre-vitellogenic resting stage by preventing apoptosis and follicle resorption in a nutrition-dependent manner (Clifton and Noriega, 2011). Although in triatomines vitellogenesis is under JH regulation (Wang and Davey, 1993; Davey, 2007), the role of this hormone on apoptosis during early follicular atresia in *D. maxima* is unknown.

During metamorphosis, some tissues or organs that not longer persist through the life of the insect are subjected to large cellular degeneration (Lockshin et al., 1981; Joza et al., 2001). There are evidences linking cell loss during larval-pupal metamorphosis with both, activation of lysosomal marker enzymes and autophagy (Goncu and Parlak, 2008; Malagoli et al., 2010). Localization of acid phosphatase by histochemstry and cytochemistry has been useful in monitoring cellular lysis and cell death in the midgut of developing *Apis mellifera* larvae (Gregorc and Bowen, 1997). During the last stage of larval development of *Manduca sexta*, fat body cells are subjected to extensive autophagy (Müller et al., 2004). More recently, it was shown that in the silkworm *B. mori*, the degradation process in the anterior silk glands during prepupal period was accompanied by increased levels of acid phosphatase, and by the

appearance of autophagic vacuoles just before the larval-pupal ecdysis (Goncu and Parlak, 2008). In *D. maxima*, follicular atresia also coursed with high levels of acid phosphatase activity (Fig. 6). However, such increases in ovarian homogenates peaked at early stages of follicle degeneration, thus preceding the distinct morphological features of autophagy clearly observed at late follicular atresia. During the regression of the larval salivary glands of *D. melanogaster*, acid phosphatase activity increased before pupation, and this biochemical pattern correlated with the discrete histochemical localization of the enzyme in intact cells. Later on, sustained acid phosphatase activation was associated with extensive cellular degeneration (Jones and Bowen, 1993). Thus, it is likely that in *D. maxima*, the high levels of acid phosphatase activity at the initial stages of atresia may be an early signal for autophagy, thus preceding the appearance of ultrastructural signs of cell lysis.

Autophagy is a conserved response to starvation in all eukaryotes, responsible for the bulk degradation of intracellular material in order to re-route the resulting macromolecules (Kabeya et al., 2004; Backues and Klionsky, 2011). However, autophagy also occurs constitutively at low levels even under nutrient-rich conditions (Mizushima and Klionsky, 2007). At molecular level, many components of the machinery involved in autophagy have been characterized and among them, LC3 is used to specifically mark autophagic compartments (Kabeya et al., 2000; Eskelinen, 2005). Although in *D. maxima* basal levels of autophagy were observed during vitellogenesis (Fig. 7E), both, the conversion of LC3-I to LC3-II and the punctate fluorescent pattern of LC3-II demonstrated the activation of autophagic cell death throughout the stage of follicular atresia. Moreover, we found that the extent of such activation was more relevant at late atresia, as indicated by the increasing amounts of LC3-II detected by western-blot and immunofluorescence assays (Fig. 7B-C). Since in *D. maxima* no signs of apoptosis were detected

at late follicular atresia stage, probably because the apoptotic program is close to be completed, and the fact that autophagy is enhanced by nutrient deprivation (Kourtis and Tavernarakis, 2009), it is likely that intensification of autophagy at late atresia may function more efficiently for removing follicular cell remnants. During late oogenesis in *D. virilis*, Velentzas et al. (2007a) also proposed that autophagy contributed to the rapid and efficient clearance of the nurse cell corpses from the adjacent follicular epithelium.

At present, the interplay among cell death mechanisms offers different scenarios, particularly for apoptosis and autophagy (Eisenberg-Lerner et al., 2009; Kourtis and Tavernarakis, 2009). As proposed for mammals, in some insect species both mechanisms are not mutually exclusive pathways, and they can act synergistically in order to achieve a more efficient cellular removal (Velentzas et al., 2007a,b; Eisenberg-Lerner et al., 2009). On the other hand, Nezis et al. (2009) demonstrated that autophagy can act upstream of apoptosis during early oogenesis of *D. melanogaster*. Whereas apoptosis has been reported as the major cell death mechanism occurring in ovaries in response to different types of stress such as parasite infection (Hopwood et al., 2001), mating delay, alone or in combination with starvation (Moore and Sharma, 2005; Barret et al., 2008), in *R. prolixus* both, apoptosis and autophagy were operative when atresia was induced by a fungal infection (Medeiros et al., 2011). On the contrary, in *D. maxima* we showed that apoptosis, autophagy and necrosis operated during follicular atresia induced by blood meal deprivation during post-vitellogenesis. Moreover, it was shown that these cell death mechanisms correlated with the progression of the degenerative process, thus, apoptosis played a major role during early atresia, and autophagy and necrosis seemed to be more relevant at late stages of the process. Although it is complex to determine the nature of the cross-talk among these cell death mechanisms in *D. maxima,* it is possible that at early atresia,

the simultaneous occurrence of apoptosis and autophagy would allow a selective cell removal, with no severe consequences to most of the ovarian tissue. In the context of the physiology of *D. maxima*, this process would facilitate another oviposition cycle if females accessed to a blood source. In this vector, as in all triatomines, at least for a second batch of eggs, the blood meal is needed to resume vitellogenesis (Stoka et al., 1987). In fact, under standardized conditions, the females of *D. maxima* can take a second blood meal between 5-7 days after the oviposition period has ceased to successfully resume vitellogenesis (Aguirre et al., 2011). At late atresia, however, even if the nutritional condition is reverted, the pronounced morphological changes promoted by autophagy and necrosis may render the ovaries less competent to accomplish a new oviposition cycle, prioritizing the utilization of resources to increase female lifespan. Further studies directed to evaluate the signaling pathways of apoptosis and autophagy will contribute to determine the interplay of such cell death mechanisms during the process of follicular atresia.

5. Acknowledgements

We thank Dr. E. R. Rubiolo and Dr. L. L. Fruttero for critical reading of the manuscript and for their helpful suggestions throughout the course of the work. The authors are grateful to Dr. P. Iribarren for the cleaved caspase-3 antibody and R. Stariolo (Coordinación Nacional de Control de Vectores, Córdoba, Argentina) for rearing of insects. This work was supported by Grants from FONCyT (PICT 2007-01333, ANPCyT-Argentina), Consejo Nacional de Investigaciones Científicas y Técnicas (PIP 2011/13-CONICET) and SECyT-UNC. The experiments of this work were performed during the tenure of a PGII-CONICET fellowship awarded to S.A.A.

6. References

Aguirre, S.A., Frede, S., Rubiolo, E.R., Canavoso, L.E., 2008. Vitellogenesis in the hematophagous *Dipetalogaster maxima* (Hemiptera: Reduviidae), a vector of Chagas' disease. Journal of Insect Physiology 54, 393-402.

Aguirre, S.A., Fruttero, L.L., Leyria, J., Defferrari, M.S., Pinto, P.M., Settembrini, B.P., Rubiolo, E.R., Carlini, C.R., Canavoso, L.E., 2011. Biochemical changes in the transition from vitellogenesis to follicular atresia in the hematophagous *Dipetalogaster maxima* (Hemiptera: Reduviidae). Insect Biochemistry and Molecular Biology 42, 832-841.

Backues, S.K., Klionsky, D.J., 2011. Autophagy gets in on the regulatory act. Journal of Molecular Cell Biology 3, 76-77.

Barrett, E.L., Preziosi, R.F., Moore, A.J., Moore, P.J., 2008. Effects of mating delay and nutritional signals on resource recycling in a cyclically breeding cockroach. Journal of Insect Physiology 54, 25-31.

Bell, W.J., Bohm, M.K., 1975. Oosorption in insects. Biological Reviews of the Cambridge Philosophical Society 50, 373-396.

Canavoso, L.E., Rubiolo, E.R., 1995. Interconversions of lipophorin particles by adipokinetic hormone in hemolymph of Panstrongylus megistus, *Dipetalogaster maximus* and *Triatoma infestans* (Hemiptera: Reduviidae). Comparative Biochemistry and Physiology 112A, 143-150.

Clifton, M.E., Noriega, F.G., 2011. Nutrient limitation results in juvenile hormone-mediated resorption of previtellogenic ovarian follicles in mosquitoes. Journal of Insect Physiology 57, 1274-1281.

Coura, J.R; Viñas, P.A., 2010. Chagas disease: a new worldwide challenge. Nature 465, S6-S7.

Davey, K., 2007. The interaction of feeding and mating in the hormonal control of egg production in *Rhodnius prolixus*. Journal of Insect Physiology 53, 208-215.

Eisenberg-Lerner, A., Bialik, S., Simon, H.U., Kimchi, A., 2009. Life and death partners: apoptosis, autophagy and the cross-talk between them. Cell Death and Differentiation 16, 966-975.

Eskelinen, E.L. 2005. Maturation of autophagic vacuoles in mammalian cells. Autophagy 1, 1-10.

Fruttero, L.L., Rubiolo, E.R., Canavoso, L.E., 2009. Biochemical and cellular characterization of lipophorin-midgut interaction in the hematophagous *Panstrongylus megistus* (Hemiptera: Reduviidae). Insect Biochemistry and Molecular Biology 39, 322-331.

Galluzzi, L., Maiuri, M.C., Vitale, I., Zischka, H., Castedo, M., Zitvogel, L., Kroemer, G., 2007. Cell death modalities: classification and pathophysiological implications. Cell Death and Differentiation 14, 1237-1243.

Gavrieli, Y., Sherman, Y., Ben-Sasson, S.A., 1992. Identification of programmed cell death in situ via specific labeling of nuclear DNA fragmentation. Journal of Cell Biology 119, 493-501.

Golstein P., Kroemer G., 2005. Redundant cell death mechanisms as relics and backups. Cell Death and Differentiation 12, 1490-6.

Golstein, P., Kroemer, G., 2007. Cell death by necrosis: towards a molecular definition. Trends in Biochemical Science 32, 37-43.

Goncu, E., Parlak, O., 2008. Some autophagic and apoptotic features of programmed cell death in the anterior silk glands of the silkworm, *Bombyx mori*. Autophagy 4, 1069-1072.

Gregorc, A., Bowen, I.D., 1997. Programmed cell death in the honey-bee (*Apis mellifera L.*) larvae midgut. Cell Biology International 21, 151-158.

Hopwood, J.A., Ahmed, A.M., Polwart, A., Williams, G.T., Hurd, H., 2001. Malaria-induced apoptosis in mosquito ovaries: a mechanism to control vector egg production. The Journal of Experimental Biology 204, 2773-2780.

Huebner, E., Anderson, E., 1972. A cytological study of the ovary of *Rhodnius prolixus*. Oocyte differentiation. Journal of Morphology 137, 385-416.

Jones, H.E., Bowen, I.D., 1993. Acid phosphatase activity in the larval salivary glands of developing *Drosophila melanogaster*. Cell Biology International 17, 305-315.

Joza, N., Susin, S.A., Daugas, E., Stanford, W.L., Cho, S.K., Li, C.Y., Sasaki, T., Elia, A.J., Cheng, H.Y., Ravagnan, L., Ferri, K.F., Zamzami, N., Wakeham, A., Hakem, R., Yoshida, H., Kong, Y.Y., Mak, T.W., Zúñiga-Pflücker, J.C., Kroemer, G., Penninger, J.M., 2001. Essential role of the mitochondrial apoptosis-inducing factor in programmed cell death. Nature 410, 549-54.

Kabeya, Y., Mizushima, N., Ueno, T., Yamamoto, A., Kirisako, T., Noda, T., Kominami, E., Ohsumi, Y., Yoshimori, T., 2000. LC3, a mammalian homologue of yeast Apg8p, is localized in autophagosome membranes after processing. The EMBO Journal 19, 5720-5728.

Kabeya, Y., Mizushima, N., Yamamoto, A., Oshitani-Okamoto, S., Ohsumi, Y., Yoshimori, T., 2004., LC3, GABARAP and GATE16 localize to autophagosomal membrane depending on form-II formation. Journal of Cell Science 117, 2805-12.

Kerr, J.F.R., Wyllie, A.H., Currie, A.R., 1972. Apoptosis: a basic biological phenomenon with wide- ranging implications in tissue kinetics. British Journal of Cancer 26, 239-257.

Köhler, C., Orrenius, S., Zhivotovsky, B., 2002. Evaluation of caspase activity in apoptotic cells. Journal of Immunological Methods 265, 97-110.

Klionsky, D.J, Abeliovich, H., Agostinis, P., Agrawal, D.K., Aliev, G., Askew, D.S., Baba, M., Baehrecke, E.H., Bahr, B.A., Ballabio, A., Bamber, B.A., Bassham, D.C., Bergamini, E., Bi, X., Biard-Piechaczyk, M., Blum, J.S., Bredesen, D.E., Brodsky, J.L., Brumell, J.H., Brunk, U.T., Bursch, W., Camougrand, N. et al., 2008. Guidelines for the use and interpretation of assays for monitoring autophagy in higher eukaryotes. Autophagy 4, 151-175.

Kourtis, N., Tavernarakis, N., 2009. Autophagy and cell death in model organisms. Cell Death and Differentiation 16, 21-30.

Kroemer, G., Galluzzi, L., Vandenabeele, P., Abrams, J., Alnemri, E.S., Baehrecke, E.H., Blagosklonny, M.V., El-Deiry, W.S., Golstein, P., Green, D.R., Hengartner, M., Knight, R.A., Kumar, S., Lipton, S.A., Malorni, W., Nuñez, G., Peter, M.E., Tschopp, J., Yuan, J., Piacentini, M., Zhivotovsky, B., Melino, G., 2009. Classification of cell death: recommendations of the Nomenclature Committee on Cell Death. Cell Death and Differentiation 16, 3-11.

Lavrik, I.N., Golks, A., Krammer, P.H., 2005. Caspases: pharmacological manipulation of cell death. The Journal of Clinical Investigation 1150, 2665-2672.

Li, H., Kolluri, S.K., Gu, J., Dawson, X.C., Hobbs, P.D., Lin, B., Chen, G., Lu, J., Lin, F., Xie, Z., Fontana, J.A., Reed, J.C., Zhang, X., 2000. Cytochrome c release and apoptosis induced by mitochondrial targeting of nuclear orphan receptor TR3. Science 289, 1159-1164.

Lockshin, R.A., Beaulaton, J., 1981. Cell death: questions for histochemists concerning the causes of the various cytological changes. Histochemistry 13, 659-666.

Malagoli, D., Abdalla, F. C., Cao, Y., Feng, Q., Fujisaki, K., Gregorc, A., Matsuo, T., Nezis, I.P., Papassideri, I.S., Sass, M., Silva-Zacarin, E.C., Tettamanti, G., Umemiya-Shirafuji, R., 2010. Autophagy and its physiological relevance in arthropods: Current knowledge and perspectives. Autophagy 6, 575-88.

Matsuda, F., Inoue, N., Manabe, N., Ohkura, S., 2012. Follicular growth and atresia in mammalian ovaries: regulation by survival and death of granulose cells. Journal of Reproduction and Development 58,44-50.

Medeiros, M.N., Ramos, I.B., Oliveira, D.M., da Silva, R.C., Gomes, F.M., Medeiros, L.N., Kurtenbach, E., Chiarini, L.B., Masuda, H., de Souza, W., Machado, E.A., 2011. Microscopic and molecular characterization of ovarian follicle atresia in *Rhodnius prolixus Stähl* under immune challenge. Journal of Insect Physiology 57, 945-953.

Mizushima, N., Klionsky, D.J., 2007. Protein turnover via autophagy: implications for metabolism. Annual Review of Nutrition 27, 19-40.

Moore, P.J., Sharma, S., 2005. A delay in age at first mating results in the loss of future reproductive potential via apoptosis. Evolution & Development 7, 216-222.

Moore, P.J., Attisano, A., 2011. Oosorption in response to poor food: complexity in the trade-off between reproduction and survival. Ecology and Evolution 1, 37-45.

Mpakou, V.E., Nezis, I.P., Stravopodis, D.J., Margaritis, L.H., Papassideri, I.S., 2006. Programmed cell death of the ovarian nurse cells during oogenesis of the silkmoth *Bombyx mori.* Development, Growth & Differentiation 48, 419-428.

Müller, F., Adori, C., Sass, M., 2004. Autophagic and apoptotic features during programmed cell death in the fat body of the tobacco hornworm (*Manduca sexta).* European Journal of Cell Biology 83, 67-78.

Nezis, I.P., Stravopodis, D.J., Papassideri, I., Robert-Nicoud, M., Margaritis, L.H., 2000. Stage-specific apoptotic patterns during *Drosophila* oogenesis. European Journal of Cell Biology 79, 610-620.

Nezis, I.P., Stravopodis, D.J., Papassideri, I., Robert-Nicoud, M., Margaritis, L.H., 2002. The dynamics of apoptosis in the ovarian follicle cells during the late stages of *Drosophila* oogenesis. Cell and Tissue Research 307, 401-409.

Nezis, I.P., Stravopodis, D.J., Papassideri, I.S., Stergiopoulos, C., Margaritis, L.H., 2005. Morphological irregularities and features of resistance to apoptosis in the dcp-1/pita double mutated egg chambers during *Drosophila* oogenesis. Cell Motility and the Cytoskeleton 60, 14-23.

Nezis, I.P., Stravopodis, D.J., Margaritis, L.H., Papassideri, I.S., 2006. Follicular atresia during *Dacus oleae* oogenesis. Journal of Insect Physiology 52, 282-90.

Nezis, I.P., Lamark, T., Velentzas, A.D., Rusten, T.E., Bjørkøy, G., Johansen, T., Papassideri, I.S., Stravopodis, D.J., Margaritis, L.H., Stenmark, H., Brech, A., 2009. Cell death during *Drosophila melanogaster* early oogenesis is mediated through autophagy. Autophagy 5, 298-302.

Oliveira, D.M., Machado, E.A., 2006. Characterization of a tyrosine phosphatase activity in the oogenesis of *Periplaneta Americana.* Archives of Insect Biochemistry and Physiology 63, 24-35.

Soller, M., Bownes, M., Kubli, E., 1999. Control of oocyte maturation in sexually mature *Drosophila* females. Developmental Biology 208, 337-351.

Stoka, A.M., Salomón, O.D., Noriega, F.G., 1987. Physiology of Triatominae's reproduction. In: Brenner, R.B., Stoka, A.M. (Eds.), Chagas' Disease Vectors, vol. 2. CRC Press, Florida, pp. 109–129.

Taatjes, D.J., Sobel, B.E., Budd, R.C., 2008. Morphological and cytochemical determination of cell death by apoptosis. Histochemistry and Cell Biology 129, 33-43.

Terashima, J., Takaki, K., Sakurai, S., Bownes, M., 2005. Nutritional status affects 20-hydroxyecdysone concentration and progression of oogenesis in *Drosophila melanogaster*. Journal of Endocrinology 187, 69-79.

Tilly, J.L., 1996. Apoptosis and ovarian function. Reviews of Reproduction 1, 162-172.

Tilly, J.L., 2001. Commuting the death sentence: how oocytes strive to survive. Nature Reviews Molecular Cell Biology 2, 838-48.

Towbin, H., Stahelin, T., Gordon, J., 1979. Electrophoretic transfer of proteins from polyacrylamide gels to nitrocellulose sheets: procedure and some applications. Proceedings of the National Academy of Sciences of the United States of America 76, 4350–4354.

Uchida, K., Nishizuka, M., Ohmori, D., Ueno, T., Eshita, Y., Fukunaga, A., 2004. Follicular epithelial cell apoptosis of atretic follicles within developing ovaries of the mosquito *Culex pipiens pallens*. Journal of Insect Physiology 50, 9030-912.

Velentzas, A.D., Nezis, I.P., Stravopodis, D.J., Papassideri, I.S., Margaritis, L.H., 2007a. Mechanisms of programmed cell death during oogenesis in *Drosophila virilis*. Cell and Tissue Research 327, 399-414.

Velentzas, A.D., Nezis, I.P., Stravopodis, D.J., Papassideri, I.S., Margaritis, L.H., 2007b. Stage-specific regulation of programmed cell death during oogenesis of the medfly *Ceratitis capitata* (Diptera, Tephritidae). The International Journal of Developmental Biology 51, 57-66.

Wang, Z., Davey, K.G., 1993. The role of juvenile hormone in vitellogenin production in *Rhodnius prolixus*. Journal of Insect Physiology 39, 471–476.

Wigglesworth, V.B., 1943. The fate of the hemoglobin in *Rhodnius prolixus* and other blood-sucking arthropods. Proceedings of the Royal Society of London B 131, 313–339.

7. Figure captions

Fig. 1: Length of ovarioles and terminal follicles throughout the reproductive cycle of *D. maxima*. Sizes were registered before the fixation of the tissues and the results are expressed as mean ± SEM (n=6). (a) $P<0.001$ vs. pre-vitellogenesis, early and late atresia; (b) $P<0.01$ vs. early and late atresia; (c) $P<0.001$ vs. early and late atresia. [#] During pre-vitellogenic stage, it was not possible to distinguish a terminal follicle from the ovariole.

Fig. 2: Morphological changes in the ovaries of *D. maxima* at early follicular atresia stage (days 10-12 post-vitellogenesis). **(A)** Stereo-microscope micrograph of the ovarioles maintaining some degree of asynchronous development. Arrows indicate the presence of follicles undergoing incipient degeneration. Arrowheads show resorbed oocytes. **(B)** H&E staining of an ovarian follicle undergoing incipient degeneration. Image shows at higher magnification the area of the box indicated in the insert. Note the chromatin condensation of some nuclei (arrows) while other follicular cells show euchromatic nuclei (arrowheads). **(C)** DAPI staining showing nuclei of some follicular cells with chromatin condensation (arrows) coexisting with others lacking a chromatin condensation pattern. **(D)** Semi-thin section of ovarian tissue showing the loss of the regular array of the follicular epithelium. Follicular cells exhibit cytoplasm vacuolization (arrows) and nuclei show chromatin condensation (arrowhead). **(E)** Transmission electron micrograph (TEM) of the follicular epithelium showing a nucleus with condensed chromatin (arrow) next to another one with a normal distribution of the chromatin. **(F)** TEM micrograph of follicular cells showing apoptotic bodies (arrows) as well as a large vacuole with electron-dense

materials (open arrow). Fd, follicle undergoing incipient degeneration; Oo, oocyte; RO, resorbed oocyte; FE, follicular epithelium; N, nucleus. Bars: (A) = 400 μm, (B-D) = 10μm, (E-F) = 5 μm.

Fig. 3: Morphological changes in the ovaries of *D. maxima* at late follicular atresia stage (days 30-32 post-vitellogenesis). **(A)** Stereo-microscope micrograph showing ovarioles lacking of asynchronism. Small terminal follicles (arrows) and resorbed oocytes (arrowheads) are shown in the image. **(B)** H&E staining of an ovarian tissue section showing the unorganized follicular epithelium surrounding a small terminal oocyte. **(C)** DAPI staining of the follicular epithelium surrounding a terminal oocyte without any sign of chromatin condensation. Insert is the corresponding DIC image of (C) at lower magnification. **(D-F)** Transmission electron micrographs of follicular cells. Note the presence of a large vacuole containing remnants of organelles and a multilamellar body, evidenced as whorls of concentric membrane (**D**). The bilayered nuclear membrane shows dilation (arrow) and mitochondria lack cristae (**E**). Follicular epithelium also displayed signs of necrosis such as electron lucent vacuoles (arrows) (**F**). FE, follicular epithelium; RO, resorbed oocyte; Tf, terminal follicle; Oo, oocyte; Va, vacuole; ER, endoplasmic reticulum; M, mitochondria; MLB, multilamellar body; N, nucleus. Bars: (A) = 400μm, (B) = 20μm, (C) = 10μm, (D) = 2μm, (E) =1μm, (F) = 5μm.

Fig. 4: Micrographs of TUNEL labeling performed in ovarian tissue sections of *D. maxima*. **(A)** At early atresia stage, the TUNEL-positive labeling (arrows) was found in some follicular cells of the follicle undergoing incipient degeneration. **(B)** At vitellogenic stage, no TUNEL-positive signal was detected in the follicular epithelium. The squared areas in the inserts indicate at lower

magnification the tissue sections shown in (A) and (B). Fd, follicle undergoing incipient degeneration; Oo, oocyte; FE, follicular epithelium. Bars: 10 μm.

Fig. 5: Detection of active caspase-3 in ovarian tissue of *D. maxima* at early follicular atresia stage. Tissue sections were stained with anti-cleaved caspase-3 antibody (red) and counterstained with DAPI (blue). **(A)** Laser scanning confocal micrographs showing an intense fluorescent signal in the epithelium of follicles undergoing incipient degeneration (arrows). **(B)** DAPI staining showing follicular cells with condensed chromatin (arrowheads). **(C)** Merged images of **(A)** and **(B)** showing that the follicular cells positive for cleaved caspase-3 also exhibited chromatin condensation when stained with DAPI (asterisk). Bars: 10 μm.

Fig. 6: Acid phosphatase activity in ovarian tissue homogenates throughout the reproductive cycle of *D. maxima*. The specific activity was determined by the hydrolysis of the substrate *p*-nitrophenyl phosphate (pNPP) to *p*-nitrophenol (pNP), in a reaction mixture containing 30 μg of protein homogenates as stated in Materials and Methods. Specific activity is expressed as nmol of pNP/mg protein homogenate/min. Results are expressed as mean ± SEM (n=4). (a) $P< 0.01$ vs. pre-vitellogenesis, vitellogenesis and days 40-45 post-vitellogenesis; (b) $P< 0.001$ vs. pre-vitellogenesis, vitellogenesis and days 40-45 post-vitellogenesis; (c) $P< 0.05$ vs. days 6-8 and 30-32 post-vitellogenesis; (d) $P< 0.01$ vs. pre-vitellogenesis and vitellogenesis; (e) $P< 0.05$ vs. pre-vitellogenesis, vitellogenesis and days 6-8 post-vitellogenesis.

Fig. 7: Assessment of autophagy throughout the reproductive cycle of *D. maxima* using the specific marker LC3. **(A)** The extent of autophagosome formation was evaluated by the conversion of LC3-I (cytosolic form) to LC3-II (membrane-bound autophagosome). Western blot was performed employing homogenates of ovaries sampled in pre-vitellogenesis, vitellogenesis and at early and late atresia stages. Top panel: the arrows indicate LC3-I and LC3-II. The bottom panel shows the protein loading control stained with Ponceau S. **(B-E)** Monitoring of autophagy by indirect immunofluorescence. Ovaries from females sampled throughout the reproductive cycle were incubated with an anti-LC3 antibody and processed as stated in Material and Methods. Cryostat sections were analyzed by scanning laser confocal microscopy. **(B-C)** At early and late atresia stages, respectively, follicular cells exhibited an intense punctate fluorescence pattern that corresponds to the membrane-bound form of LC3 (LC3-II). **(D-E)** No punctate immunopositive signal of LC3-II was detected during pre-vitellogenesis **(D)**, although it was rather faintly in vitellogenesis **(E)**. Inserts correspond to DIC images at lower magnifications. Fd, follicle undergoing incipient degeneration; FE, follicular epithelium; Oo, oocyte. Bars: 10 μm.

Figure 1

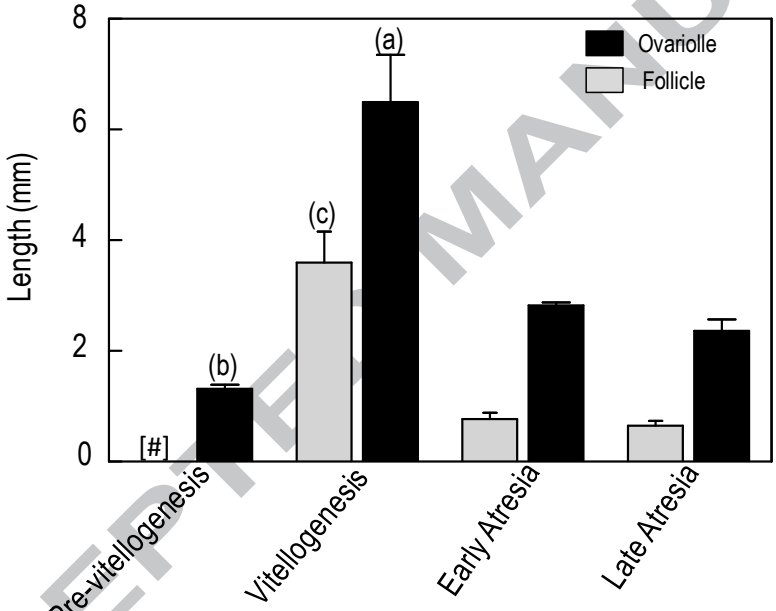

Figure 2

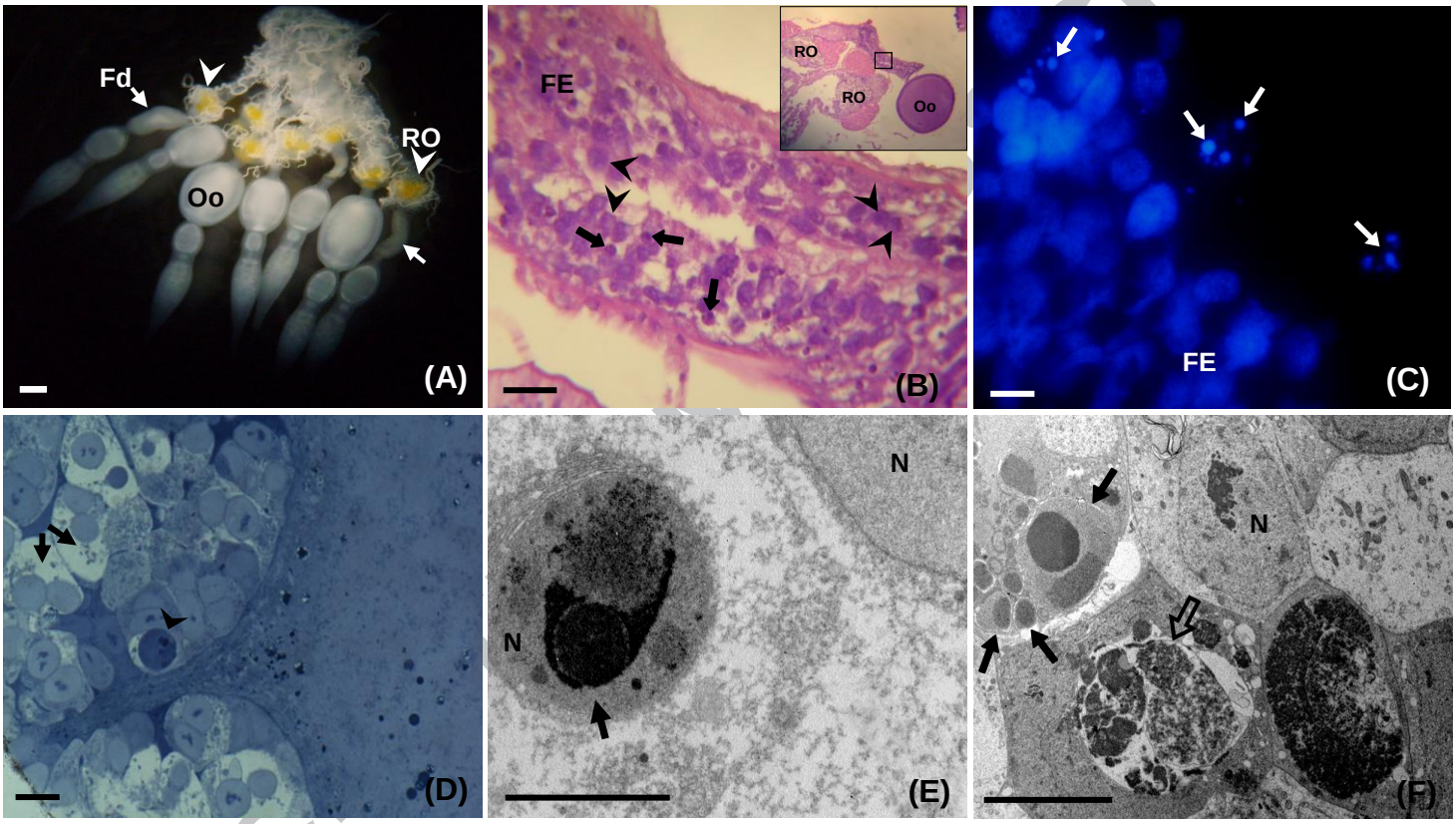

Figure 3

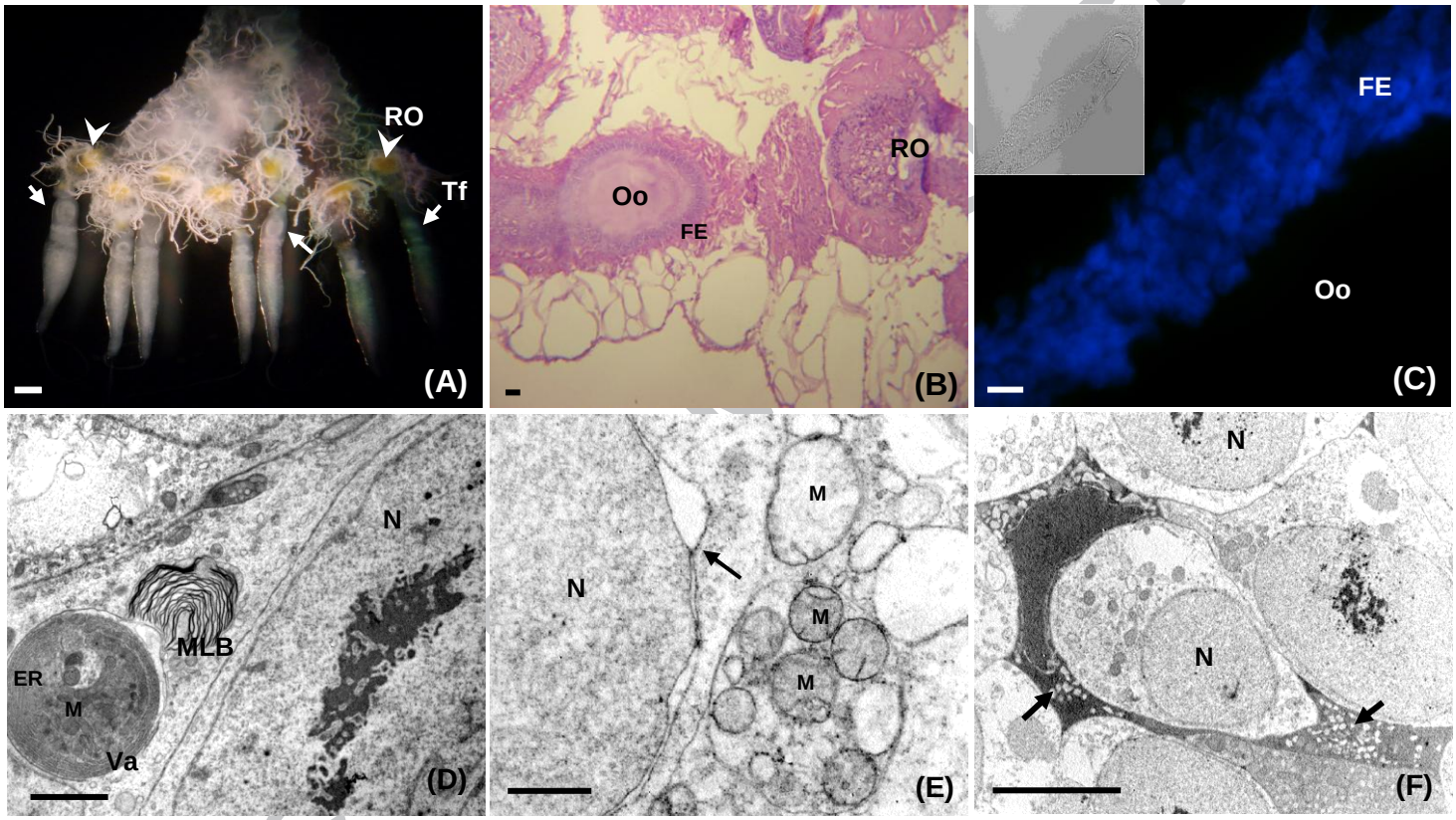

Figure 4

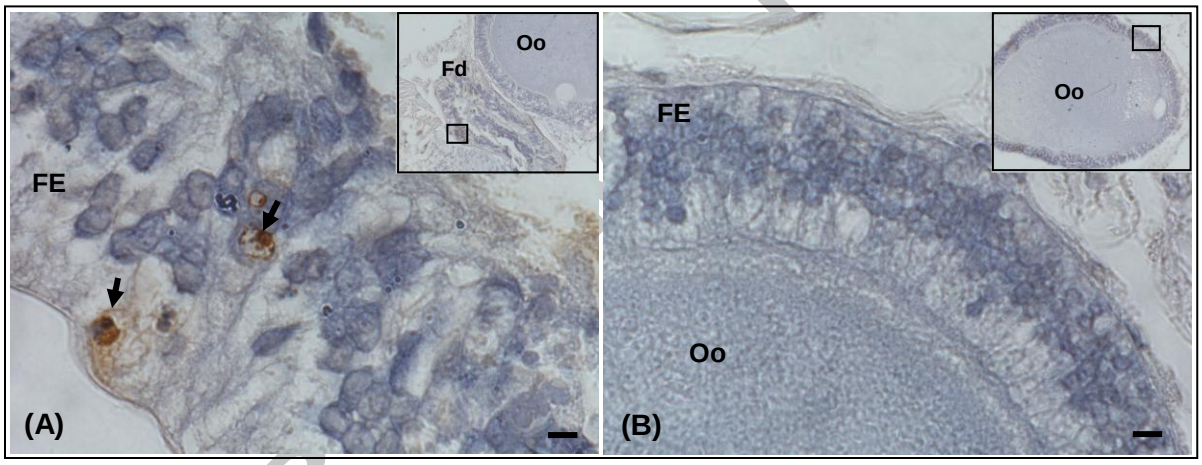

Figure 5

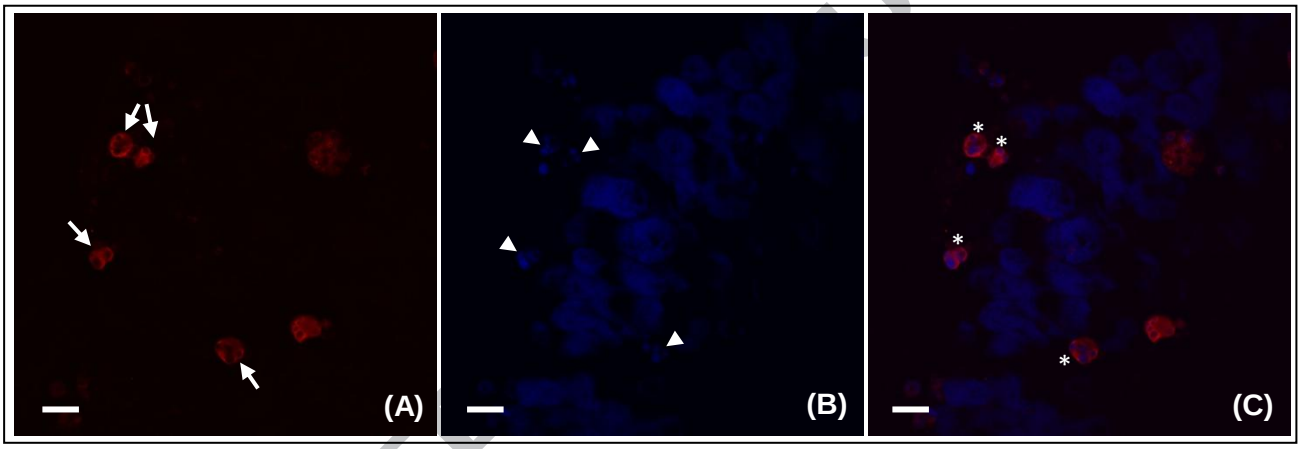

Figure 6

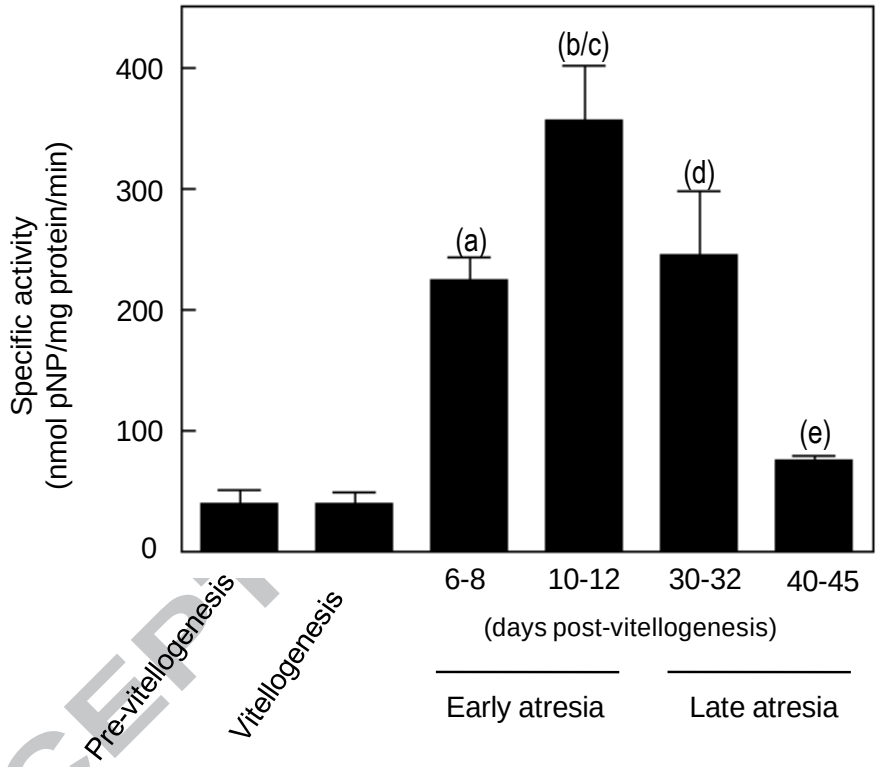

Figure 7

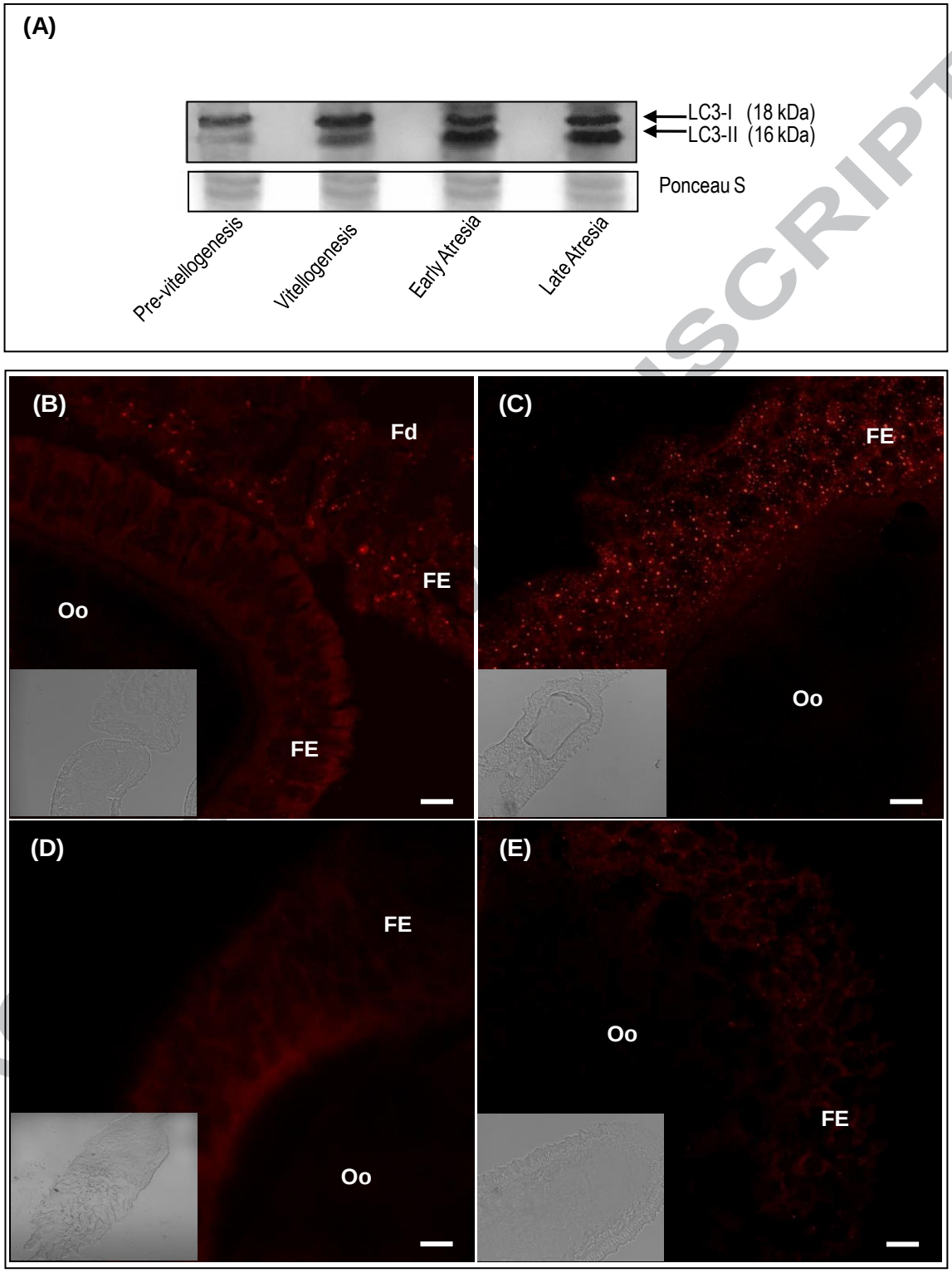

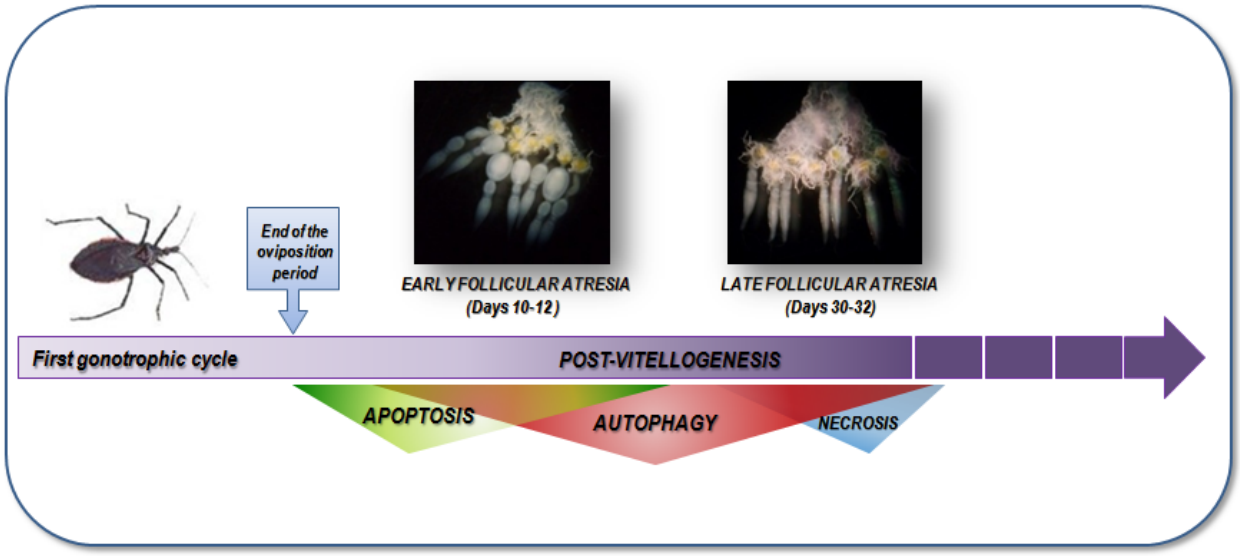

Highlights

- In early atresia, follicular cells predominantly exhibited features of apoptosis.
- High levels of acid phosphatase activity were detected in all atretic stages.
- The relevance of autophagy at late atresia was supported by cellular findings and changes on its marker.
- In late follicular atresia, cells also displayed changes compatible with necrosis.